Acta Technica 62 No. 1B/2017, 131–144

Design and kinematic control simulation of wheeled mobile table tennis manipulator

Chen Yan[1]

Abstract. The purpose of this paper is to design a wheeled mobile table tennis manipulator without the limited punching range caused by fixed arms of table tennis robots. By analyzing the structure, the technical characteristics of wheeled differential-drive mobile robot and table tennis robot are combined. In addition, kinematic control simulation is adopted to design wheeled mobile table tennis manipulator. First of all, the software and hardware exploitation platform are constructed by concerning with practical use of table tennis robot, and D-H module is also built. Moreover, the kinematics model of compartment is worked out based on the theory of building trolley module. In addition, the weighted least square method is taken as an example to solve joints limits obstacles-avoidance of mobile manipulator. The experimental results prove the validity of this method through simulation research. According to the requirements of control mission, the control method for redundant mobile manipulator is achieved. Based on the above finding, it is concluded that the relative algorithm can be used to realize the analysis on and research of sub-tasks performances characteristics.

Key words. Wheeled mobile table tennis manipulator, joint limits, D-H module, weighted least square method.

1. Introduction

1.1. Description of the problem

The commonly used mobile robot mechanisms include wheeled mobile mechanism, legged mobile mechanism, tracked mobile mechanism and wheeled legged mobile mechanism. Among them, wheeled mobile mechanism has a long history, and relatively mature in mechanical design. Therefore, in practical applications, wheeled mobile robots, or mobile manipulators, are the most important compared to other types of mobile mechanisms. The shape structure of wheeled mobile manipulator mainly consists of two parts: wheeled mobile platform and mechanical arm.

[1]Department of P. E, North China University of Water Resources and Electric Power, 450011, China

Robotics involves many disciplines like kinematics, intelligent control and bionics, whose application scope expands from industrial production to people's daily life. Among which, table tennis robots not only can perceive and precast the surroundings, but make decisions [1–3], as well as make relative combined actions. This shows advanced intellectuality, realizing automatic countermeasures in sporting events [4]. There are researches on table tennis manipulators both at home and abroad, which basically realized man-machine playing and machine-machine playing [5–6], but its real development condition is quite inferior to the practical man-man playing. For example, man can move body to catch and serve ball in a wider scope, whereas robots' fixed body only allows a very narrow range [7–8].

At present, the motion modes of mobile robots involve wheeled mode and step-mode, the latter is more difficult to control, whereas the former has a relatively advanced technology and is easier to control [9]. We based on the playing condition of mobile table tennis manipulators, made the match more similar to the man to man playing condition. We added mobile parts for the manipulators, chose 4-wheel differential-drive mobile mechanism to make research, designed wheeled mobile manipulators and proved the validity of this method through stimulation.

1.2. State of the art

The United States first proposed the concept of industrial robots, and invented the world's first industrial robot UNIMATE in 1961. Its robot technology has a long history of development and application. The Japanese robot, known as "Robot Kingdom", ranks first in the world no matter the number or density. The western European countries are also developing rapidly in the field of robotics by combining their own R & D and application. The research of mobile manipulator started earlier in foreign countries. The initial research mainly studies the architecture and information processing of outdoor robots from an academic perspective, and builds a buy test system to validate them. In the 90s, with the progress of science and technology, mobile manipulator began to develop more applications on the basis of "buy more now".

China's robot started in the early 1970s. After about 40 years of development, it has gone through three stages, from exploration, research and development to application. After several years of research, China has completed the anti nuclear reconnaissance vehicle, remote control mobile robot and wall climbing robot, and then developed anti explosion robots, eye guided vehicles and so on. Although China is a powerful country in table tennis, the research on table tennis robot started very late. The research on this aspect was first seen in the theoretical research of Shanghai Jiao Tong University in the 90s of the last century.

2. Construction of development environment

2.1. Hardware structure

We applied wheeled mobile mechanism to study the mobile manipulator in this research, whose hardware consists of compartment physical structure, dynamo, control box and CAN card [10–11]. The compartment structure of mobile manipulator applied in this research is showed in Fig. 1.

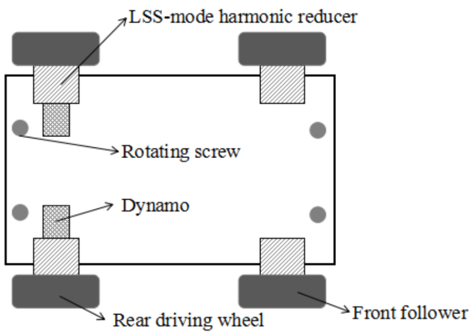

Fig. 1. Compartment structure of mobile manipulator

From Fig. 1, we can see that the compartment has 4 wheels, among which, the first two wheels are followers and the other two are driving wheels, and each one has an independent dynamo. Moreover, 4 wheels are all fixed, can only move back and forth to make the dynamo having more driving force. We utilized DC dynamo as the driving dynamo of compartment. When manipulator and dynamo are appropriately assembled, we can apply PID control to debug the dynamo(current, speed, location).

The framework diagram of debugging module is shown in Fig. 2. Input the current and peak current, after the limiting step, compare them with feedback current, and conduct PI control, then after pulse width modulation(PWM) set them as the input instruction of dynamo.

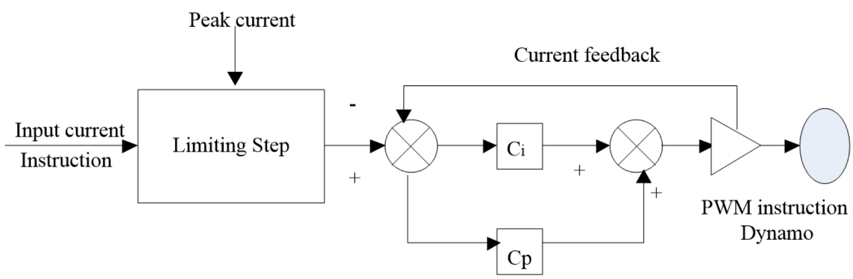

Fig. 2. Current loop debugging module of dynamo

The framework diagram of debugging module is shown in Fig. 3. After the limiting and filtering, work out the difference between the speed and feedback speed, output it through filtering after the PI control. Two times of filtering process has greatly relieved the disturbance of noise.

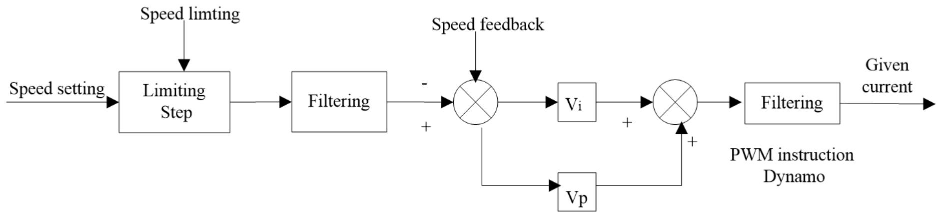

Fig. 3. Speed loop debugging module of dynamo

The framework diagram of debugging module is shown in Fig. 4. The forward circuit includes location, speed and acceleration, which can decrease error during location trailing. After debugging, the dynamo can reach a better tracing effect, laying a solid foundation for the following research.

2.2. D-H parameter

D-H (Denavit-Hartenberg) parameter includes 4 parameters: connecting rod length a_i, connecting rod corner α_i, connecting rod offset distance d_i, and articulation angle θ_i. The D-H coordinate system module is shown in Fig. 4.

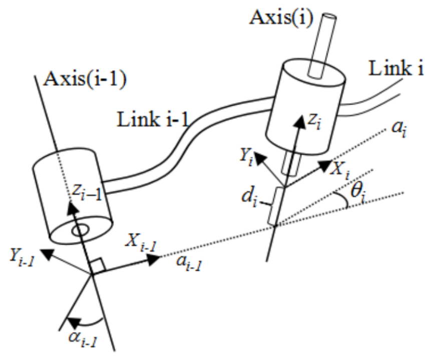

Fig. 4. D-H coordinate system module

Keep the number of a_i positive and not limiting the other three numerical values. Positive and negative values have different meanings. According to the established module, we can build various connecting rod fixed coordinate system [12–13]. The origin of fixed coordinate system can be set randomly. Choose the appropriate world coordinate system in the space based on different needs. According to the formula (1) describing the homogeneous coordinates transfer matrices on neighboring joints, we describe the space and location relationship among joints. After another transferring, work out the position of the target point in world coordination system. The formula of homogeneous coordinates transfer matrices on neighboring joints is as follows

$$
{}^{\mathrm{i-1}}_{i}T = \begin{bmatrix} \cos(\theta_i) & -\sin(\theta_i) & 0 & a_{i-1} \\ \sin(\theta_i)\cos(\alpha_{i-1}) & \cos(\theta_i)\cos\cos(\alpha_{i-1}) & -\sin\cos(\alpha_{i-1}) & -\sin\cos(\alpha_{i-1})d_i \\ \sin(\theta_i)\sin\cos(\alpha_{i-1}) & \cos(\theta_i)\sin\cos(\alpha_{i-1}) & \cos\cos(\alpha_{i-1}) & \cos\cos(\alpha_{i-1})d_i \\ 0 & 0 & 0 & 1 \end{bmatrix}. \tag{1}
$$

So the position of manipulator end to the world coordination system can be described as

$$
{}^{0}_{n}T = {}^{0}_{1}T\,{}^{1}_{2}T\,{}^{2}_{3}T \cdots {}^{n-1}_{n}T\,. \tag{2}
$$

In the formula, n refers to the number of joints.

2.3. Software development platform

We apply Visual Studio as the software development platform this time, Visual C++ as the programming language. There are two CAN cards, amounting to four channels, each has 2–3 dynamos, so we conduct programming with 4 threads.

3. Materials and methods

3.1. Kinematic modeling of the compartment

Most of mobile robots apply double-wheeled difference-drive mode, whose mobile module is shown in Fig. 5.

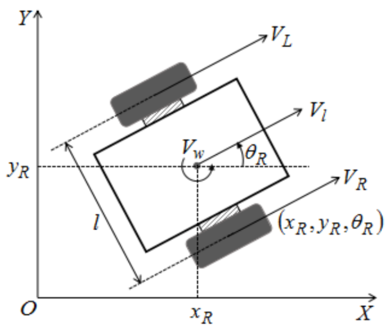

Fig. 5. Double-wheeled trolley kinematic module

In the figure, V_{L} and V_{R} refer to the left and right linear speed of two wheels respectively, l is distance of wheel shaft centers, V_{l} and V_ω are the line speed and angular speed of the trolley [14]

$$
V_{\mathrm{l}} = \frac{V_{\mathrm{L}} + V_{\mathrm{R}}}{2}, \quad V_\omega = \frac{2V_{\mathrm{R}} - V_{\mathrm{L}}}{l}\,. \tag{3}
$$

Moreover:

$$
V_{\mathrm{L}} = \omega_{\mathrm{L}} R, \quad V_{\mathrm{R}} = \omega_{\mathrm{R}} R\,. \tag{4}
$$

Here, ω_{L} and ω_{R} are the left and right angular speeds of the two wheels, respectively. And the centroid motion equation of the robot is

$$\dot{x}_R = V_{\mathrm{l}} \cos(\theta_{\mathrm{R}}), \dot{y}_{\mathrm{R}} = V_{\mathrm{l}} \sin(\theta_{\mathrm{R}}), \dot{\theta}_{\mathrm{R}} = V_{\omega}. \tag{5}$$

Given these, we can see that

$$\begin{bmatrix} \dot{x}_{\mathrm{R}} \\ \dot{y}_{\mathrm{R}} \\ \dot{\theta}_{\mathrm{R}} \end{bmatrix} = \begin{bmatrix} \frac{R \cdot \cos(\theta_{\mathrm{R}})}{2} & \frac{R \cdot \cos(\theta_{\mathrm{R}})}{2} \\ \frac{R \cdot \sin(\theta_{\mathrm{R}})}{2} & \frac{R \cdot \sin(\theta_{\mathrm{R}})}{2} \\ \frac{R}{l} & \frac{R}{l} \end{bmatrix} \begin{bmatrix} \omega_{\mathrm{R}} \\ \omega_{\mathrm{L}} \end{bmatrix}. \tag{6}$$

To simplify formula (6), conduct decoupling process. And then

$$\begin{bmatrix} \dot{x}_{\mathrm{R}} \\ \dot{y}_{\mathrm{R}} \\ \dot{\theta}_{\mathrm{R}} \end{bmatrix} = \begin{bmatrix} \cos(\theta_{\mathrm{R}}) & 0 \\ \sin(\theta_{\mathrm{R}}) & 0 \\ 0 & 1 \end{bmatrix} \begin{bmatrix} V_l \\ V_{\omega} \end{bmatrix}. \tag{7}$$

When the multi-wheeled trolley does rotational motion, there must be a center of rotation, that is instantaneous center of curvature (ICC) [15]. As to difference-drive trolley, ICC locates on the public axis of the two wheels, and can moves back and forth. The location is decided by the speed of the two wheels. The mobility model of trolley is shown in Fig. 6.

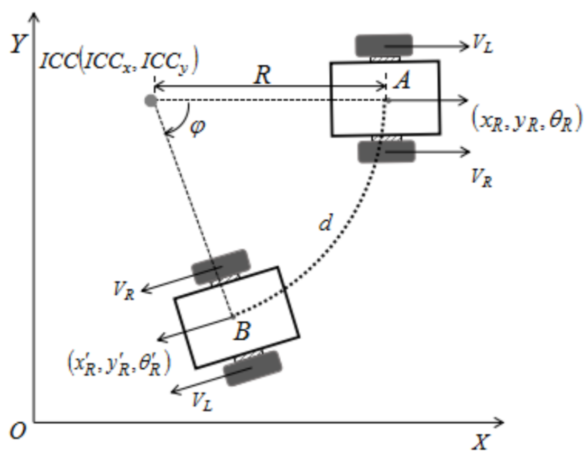

Fig. 6. Mobility model of trolley

In formula (7), R is the distance between ICC and the center of gravity A. So

$$\frac{v_{\mathrm{L}}}{v_{\mathrm{R}}} = \frac{R - \frac{l}{2}}{R + \frac{l}{2}} \rightarrow R = \frac{l}{2} \frac{v_{\mathrm{R}} + v_{\mathrm{L}}}{v_R - v_L}. \tag{8}$$

When the trolley makes direct linear movement, $v_{\mathrm{R}} = v_{\mathrm{L}}$, when $v_{\mathrm{R}} \neq v_{\mathrm{L}}$, the trolley makes rotational motion. When the time is t, trolley moves from A, after the time length of εt, it moves to B. ICC can be calculated as follows:

$$\mathrm{ICC} = [\mathrm{x_R} - R\sin(\theta_{\mathrm{R}}), y_{\mathrm{R}} + R\cos(\theta_{\mathrm{R}})] \ . \tag{9}$$

According to $(1+\varepsilon)t$ and the angular speed $v_{\omega'}$, we can work out the position of B:

$$\begin{bmatrix} x'_{\mathrm{R}} \\ y'_{\mathrm{R}} \\ \theta'_{\mathrm{R}} \end{bmatrix} = \begin{bmatrix} \cos(\omega\varepsilon t) & \sin(\omega\varepsilon t) & 0 \\ \sin(\omega\varepsilon t) & \cos(\omega\varepsilon t) & 0 \\ 0 & 0 & 1 \end{bmatrix} . \tag{10}$$

In the same way, the motion distance d and rotating anger ϕ can be worked out:

$$d = \int_t^{t+\varepsilon t} v_1 \,\mathrm{d}t = \int_t^{t+\varepsilon t} \frac{v_{\mathrm{L}} + v_{\mathrm{R}}}{2} \,\mathrm{d}t \,, \tag{11}$$

$$\phi = \frac{d}{R} = \frac{\int_t^{t+\varepsilon t} (v_{\mathrm{L}} + v_{\mathrm{R}}) \,\mathrm{d}t}{l\,(v_{\mathrm{L}} + v_{\mathrm{R}})} (v_{\mathrm{R}} - v_{\mathrm{L}}) \ . \tag{12}$$

Given these, we can work out the linear speed v_{L} and v_{R} of the two wheels, and the angular speed v_ω of the trolley.

4. Trajectory planning of mobile manipulator

The trajectory planning of mobile manipulator refers to working out the reserved trajectory concerning with the relative kinematic knowledge and the requirements of controlling task. The controlling task may be the mobility of a certain joint of the manipulator, or the concrete mobility in space.

The trajectory planning process can be seen in Fig. 7. During the serving process, there are two different plannings, one is task space planning when serving the ball, the other one is joint space planning when restoring. The interpolation algorithm of these two plannings are not the same. See the following for more details.

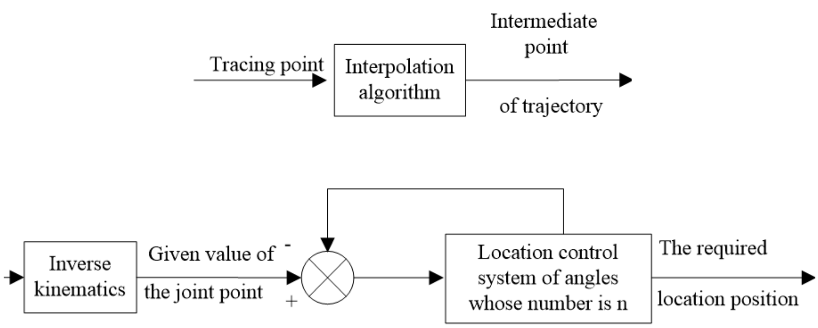

Fig. 7. Trajectory planning of mobile manipulator

We will introduce task space planning with the method of cubic polynomial interpolation, which can be classified into with and without intermediate point. If we want to work out the cubic polynomial interpolation, there must be 4 known conditions, or constraint conditions: the angle and speed limit at two positions.

Without passing intermediate point, if the angle constraint of two positions are within the range of joint limit, the speed constraint is 0. If the starting motion point of every joint is t_i, the joint angle is θ_i. If the ending point is t_e, the joint angle is θ_e. Then

$$\theta(t_0) = \theta_0, \theta(t_\mathrm{e}) = \theta_\mathrm{e}; \dot{\theta}(t_0) = \dot{\theta}(t_\mathrm{e}) = 0 \tag{13}$$

and the cubic polynomial interpolation is

$$\theta(t) = A_0 + A_1 t + A_2 t^2 + A_3 t^3 \,. \tag{14}$$

Taking the derivative of $\theta(t)$, we can see the joint speed $\dot{\theta}(t)$ and joint acceleration $\ddot{\theta}(t)$. Thus, four equations on factors can be drawn out, see the following formula

$$\theta_0 = \mathrm{A}_0 \ \ , \ \ A_1 = 0 \ \ , \ \ \theta_\mathrm{e} = A_0 + A_1 t_\mathrm{e} + A_2 t_\mathrm{e}^2 + A_3 t_\mathrm{e}^3 \ \ , \ \ A_1 + A_2 t_\mathrm{e} + 3\mathrm{A}^3 t_\mathrm{e}^2 = 0 \,. \tag{15}$$

The processing of joint space trajectory is a circulated process. Therefore, we only need to make planning following the steps above to accomplish the whole motion planning.

However, passing the intermediate point can be classified into two conditions: the speed is 0 or is not 0. When the speed is 0, we can process it according to the solutions above. When it is not, we need to process it based on the following steps. So the constraint condition that needs to be changed when speed isn't 0 is:

$$\dot{\theta}(0) = \dot{\theta}_0, \dot{\theta}(t_\mathrm{e}) = \dot{\theta}_\mathrm{e} \,. \tag{16}$$

The intermediate point value produced during joint space planning when using interpolation arithmetic is the joint angle value. The intermediate point value produced during task space planning is the three-dimensional coordinate values in Cartesian space. But the mobility of manipulators are realized by the coordinated motion of many joints, during which, a large number of arithmetical operations are needed, which leads to a longer control period.

When interpolating among task space, there are two frequently-used methods: linear interpolation method–work out the relative joint angle value through inverse operation, move to realize the required trajectory, and at the same time, the continuity of various points are approved; arc interpolation arithmetic, which includes planar arc interpolation arithmetic and space arc interpolation arithmetic.

5. Results

5.1. Kinematic control method

During the practical applying, the freedom degree of manipulator is about 8, to realize the change of end position, we need 6 task vectors at most. So, manipulator is of redundancy, and can be used to accomplish some extra submissions.

The kinematic equation of manipulator is

$$x = f(q), \quad \dot{x} = J(q)\dot{q}\,. \tag{17}$$

In this formula, x is the task space vector quantity of dimension m of the manipulator, q is the joint space vector quantity of dimension n, $\dot{x}$ and $\dot{q}$ are the relative speed, f is the forward direction kinematic relation of them, $J\,(q)$ is the Jacobian matrix in line m list n.

When $m < n$, the mobile manipulator is a redundant manipulator, resulting in non numerous inverse solution of formula (17). However, there are many methods to accomplish the control on mobile manipulator, whose frequent subtasks are a large number. We work out this equation by choosing weighted least square method and by which to solve joint limits and avoid problems.

The expected result of this research: when the joint of manipulator is close to joint limits, constraint the subtask of joint obstacles-avoidance to ensure the safety of its hardware. When the joint is far away from the joint limits, do not constraint the subtasks any more, thus to ensure the realize of main tasks, and gain a well accuracy in end task control.

The operation plan of weighted least square method is: introduce matrix and vector quantity to meet the equation

$$J_{\mathrm{w}} = JW^{-\frac{1}{2}}, \; \dot{q}_{\mathrm{w}} = W^{\frac{1}{2\dot{q}}}\,. \tag{18}$$

Here, $W \in R^{n\times n}$ is symmetric positive-definite weighted matrix, we can work out that

$$\dot{x} = J\dot{q} = J_{\mathrm{w}}\dot{q}_{\mathrm{w}}\,. \tag{19}$$

If the Jacobian matrix is nonsingular, then the weighted least square solution of formula (19) is:

$$\dot{q} = W^{-1}J^{\mathrm{T}}\left(JW^{-1}J^{\mathrm{T}}\right)^{-1}\dot{x}\,. \tag{20}$$

As to joint obstacles-avoidance, there is:

$$H\,(q) = \sum_{i=1}^{n} \frac{(q_{\mathrm{u}} - q_{\mathrm{d}})^2}{4(q_{\mathrm{u}} - q_{\mathrm{i}})(q_{\mathrm{i}} - q_{\mathrm{d}})}\,. \tag{21}$$

In this formula, q_{i} is the number i joint angle, q_{u} and q_{d} are the upper and lower limits of the mobility range of joints respectively.

5.2. Simulation experiment

Let (x_0, y_0, z_0) refer to world coordinated system and (x_1, y_1, z_1) be the coordinate system of mobile joints. The left 7 are the coordinate system of 7 joints of the manipulator. The relative D-H parameter is shown in Table 1.

Now we will conduct simulation study on joint limits avoidance through weighted least square method. If the initial joint position is

$$q_i = [0.26\ \ 200\ \ 90\ \ 80\ \ 250\ \ 105\ \ 180\ \ 135]\ ,$$

where the unit of 0.26 is "m", the others are "°". Then, the relative joint position is

$$^0T_{8i} = \begin{bmatrix} 0.0502 & 0.1855 & 0.9811 & 0.3304 \\ 0.2005 & -0.9638 & 0.1722 & 0.8396 \\ 0.9779 & 0.1880 & -0.0853 & 0.2571 \\ 0 & 0 & 0 & 1 \end{bmatrix} .$$

Table 1. D-H parameter

Joint	J1	J2	J3	J4	J5	J6	J7	J8
Rotation angle α (°)	0	90	90	90	90	90	0	90
Connecting rod length a (mm)	0	0	0	0	0	0	1.2	0
Connecting rod deflection distance d (mm)	0.26*	68	5	156	325	-5	0	0
Joint angle θ (°)	90#	0	180	180	90	180	180	90

Note: *is variation and # is fixed value.

Its position in task space is

$$x(0) = [0.4776\ \ \ 0.8652\ \ \ 0.2443\ \ \ 0.2083\ \ \ 1.3247]\ .$$

The whole motion cycle is 4 s, and the objective position of task space is

$$x(4) = [0.5501\ \ \ 1.0647\ \ \ 0.3998\ \ \ 0.4699\ \ \ 1.0528]\ .$$

The results are shown in Figs. 8–10. In Fig. 8 we can see that the whole motion process is steady and soft, realizing joint avoidance. Figure 9 shows that the speed changes smoothly during the whole process of motion, and without reaching the joint speed limits. From Fig. 10 we can see that the error precision of trailing the main task is 10^{-3}, accomplishing both the main task and subtask of joint obstacles–avoidance.

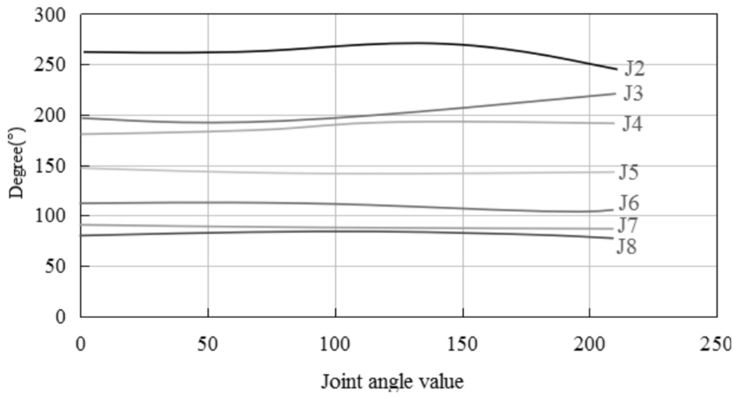

Fig. 8. Joint location (the horizontal axis is joint angle value, vertical axis is degree, i.e."°"

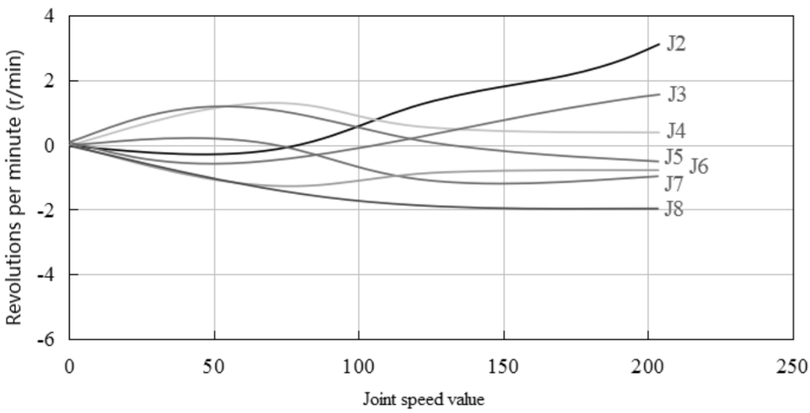

Fig. 9. Relationship of joint speed and revolutions per minute

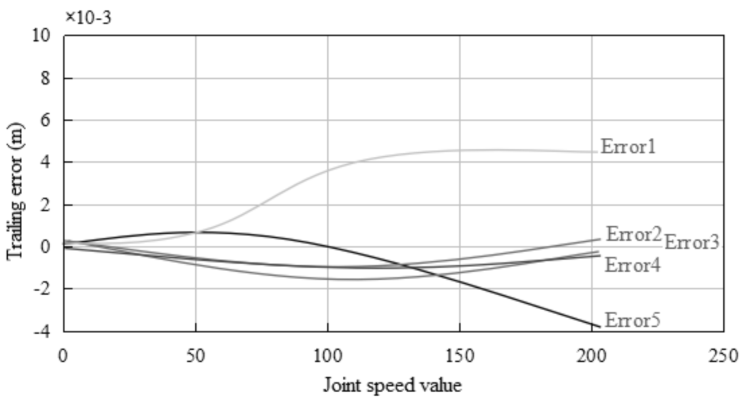

Fig. 10. Trailing error of the main task of joint limits avoidance

6. Conclusion

Based on the experimental results for the wheeled mobile table tennis manipulator, the mobile parts of the manipulators are designed to construct the whole mobile manipulator. From the perspective of freedom range, it is proved that mobile manipulator improves its redundancy and the flexibility when processing subtasks like joints obstacles-avoidance, space obstacles-avoidance and so on. In addition, the weighted least square method is selected to complete the research on subtask of the manipulator (joint limits obstacles-avoidance), which proves the validity of this method. Moreover, it is concluded that the heavy weight of the mobile parts can lead to a greater movement inertia. Therefore, it is necessary to avoid moving by a large margin to control accuracy during distributing the joint speed. Meanwhile, it is believed that this problem will also be refined specifically in the following researches.

References

[1] K. Mülling, J. Kober, O. Kroemer, J. Peters: *Learning to select and generalize striking movements in robot table tennis.* The International Journal of Robotics Research *32* (2013), No. 3, 263–279.

[2] G. Campion, G. Bastin, B. D'Andrea-Novel: *Structural properties and classification of kinematic and dynamic models of wheeled mobile robots.* Journal Nelineinaya Dinamika *7* (2011), No. 4, 733–769.

[3] M. J. Hayawi, A. A. M. Isa, M. A. Anuar, A. R. Omar: *Research article kinematic and dexterity analysis of a 3-dof parallel manipulator.* Journal of Applied Sciences, Engineering and Technology *12* (2016), No. 2, 239–248.

[4] Y. D. Wang, L. W. Wang, H. W. Zhang, H. J. Dong: *Research and application for the regularity of distribution about curvature radius and curvature center of the linkage point track in a link mechanism.* International Journal of Plant Engineering and Management *17* (2012), No. 3, 160–168.

[5] S. Han, H. Ha, Y. Zhao, J. Lee: *Assumed model feedforward sliding mode control for a wheeled mobile robot with 3-DOF manipulator systems.* Journal of Mechanical Science and Technology *31* (2017), No. 3, 1463–1475.

[6] Y. C. Chang, Y. Yamamoto: *On-line path planning strategy integrated with collision and dead-lock avoidance schemes for wheeled mobile robot in indoor environments.* Industrial Robot *35* (2008), No. 5, 421–434.

[7] H. Kim, B. K. Kim: *Online minimum-energy trajectory planning and control on a straight-line path for three-wheeled omnidirectional mobile robots.* IEEE Transactions on Industrial Electronics *61* (2014), No. 9, 4771–4779.

[8] Y. D. Patel, P. M. George: *Simulation of kinematic and workspace analysis of 3-PRS parallel manipulator.* International Journal of Modeling, Simulation, and Scientific Computing *6* (2015), No. 1, paper 1550007.

[9] J. Johnson, R. Pillai, S. M. Vignesh, A. L. Srinivas: *Design and kinematic analysis of a 6-dof parallel manipulator for pharmaceutical application.* Journal of Chemical and Pharmaceutical Sciences *9* (2016), No. 4, 3283–3288.

[10] D. Liang, Y. Song, T. Sun, G. Dong: *Optimum design of a novel redundantly actuated parallel manipulator with multiple actuation modes for high kinematic and dynamic performance.* Nonlinear Dynamics *83*, (2016), Nos. 1–2, 631–658.

[11] J. Yan, X. Guo, Y. Liu, J. Zhao: *The design and kinematic analysis of a modular manipulator.* Journal of Harbin Institute of Technology *47* (2015), No. 1, 20–25.

[12] D. Zhang, B. Wei: *Design, kinematic and dynamic modeling of a novel tripod based manipulator.* Robotica *34* (2016), No. 10, 2186–2204.

[13] T. Ito, S. Takata: *Exsistance theorem and error bound of numerical solutior for optimal control problems of continuous system.* Transactions of the Society of Instrument and Control Engineers *18* (1982), No. 7, 647–652, Released (2009).

[14] Z. Shao, X. Tang, L. Wang, D. Sun: *Atlas based kinematic optimum design of the Stewart parallel manipulator*. Chinese Journal of Mechanical Engineering *28* (2015), No. 1, 20–28.

[15] C. Park, D. I. Park, D. Kim: *The analysis of trajectory tracking error caused by the tolerance of the design parameters of a parallel kinematic manipulator*. Joural of Korea Robotics Society *11* (2016), No. 4, 248–255.

Received June 29, 2017